Heart Failure Clinic,
ISSN / eISSN 1551-7136
Publisher ELSEVIER SCIENCE INC,
STE 800, 230 PARK AVE,
NEW YORK, USA, NY, 10169
Volume 26-Issue 1-(2026)
DOI:https://doi.org/10.65613/736542

High Oxalate Exacerbates Calcium Oxalate Stone-Associated Renal Injury by Regulating Macrophage Polarization via the IRF-1/miR-301/CSF-1 Axis

Zhen Wang[1], Yuantao Zhao[1] ,Qing Wang[2], Fa Sun[1,a,*],Kehua Jiang[2,b,*]
[1] Guizhou Medical University, 550000, ,Guiyang,*china*
[2] Department of Urology, Guizhou Provincial People's Hospital,550000, ,Guiyang,*china*
[a]Email:18984159914@163.com
[*]Email:gzykdx3627@163.com

Abstract

Objective:

Calcium oxalate (CaOx) stones are the most common type of kidney stones, and hyperoxaluria is a major risk factor. Although high oxalate levels are closely associated with crystal formation, the underlying molecular mechanisms remain incompletely understood. This study aims to investigate whether the IRF-1/miR-301/CSF-1 signaling axis in renal tubular epithelial cells regulates macrophage polarization and thereby contributes to CaOx crystal formation.

Methods:

Human renal tubular epithelial cells (HK-2) were stimulated with sodium oxalate (NaOx) and co-cultured with macrophages to assess macrophage polarization. IRF-1 and miR-301 were overexpressed or inhibited using plasmid transfection and oligonucleotides, respectively. The direct targeting of CSF-1 by miR-301 was validated using a dual-luciferase reporter assay. Crystal deposition was evaluated by Von Kossa staining. Expression levels of key molecules were analyzed by qRT-PCR, Western blot, immunofluorescence, and immunohistochemistry.

Results:

NaOx stimulation upregulated IRF-1 expression in HK-2 cells. When these cells were co-cultured with macrophages under oxalate treatment, macrophages polarized toward the M1 phenotype. Mechanistically, IRF-1 in HK-2 cells transcriptionally activated miR-301 expression, and CSF-1 was identified as a direct target of miR-301. Inhibition of miR-301 in HK-2 cells or supplementation with recombinant CSF-1 shifted macrophage polarization toward the M2 phenotype. These cellular findings were consistent with in vivo results: IRF-1 knockout mice exhibited reduced renal crystal deposition, decreased miR-301 expression, and increased CSF-1 levels.

Conclusion:

The IRF-1/miR-301/CSF-1 signaling axis plays a critical role in a hyperoxaluric environment by promoting M1 macrophage polarization and facilitating CaOx crystal formation. Targeting this pathway may provide new strategies for the prevention and treatment of CaOx kidney stones.

Keywords: Sodium oxalate; IRF-1; miR-301; CSF-1; Macrophage

1.Introduction

Kidney stone disease is a common urinary tract disorder, often associated with renal colic, urinary tract infections, and impaired renal function. In China, its prevalence is approximately 6.4% and continues to rise. The pathogenesis of kidney stones is not fully understood, and effective preventive measures remain limited. The 10-year recurrence rate for calcium oxalate stones, the most predominant type of kidney stones, can reach up to 50%.

Several theories have been proposed, including Randall‘s plaque theory, supersaturated crystallization, renal injury theory, and inflammation/oxidative stress theory. Recent studies have indicated a strong relationship between inflammation and CaOx crystal formation. Macrophages, as key immune cells, are significantly increased in number in the kidneys during stone formation. Macrophages exhibit two polarization states: the M1 phenotype promotes inflammation, facilitating crystal adhesion and aggregation, whereas the M2 phenotype reduces inflammation and alleviates tissue injury.

Macrophage polarization is modulated by various molecules, among which the interferon regulatory factor (IRF) family serves as important nuclear transcription factors. Previous research has demonstrated upregulated expression of IRF-1 in renal tissues of hyperoxaluric mice. However, how IRF-1 in renal tubular epithelial cells regulates macrophage polarization remains to be investigated. As a transcription factor, IRF-1 may facilitate this process by modulating downstream molecules.

MicroRNAs are important regulators of gene expression that bind to the 3′-untranslated region (3′-UTR) of target mRNAs to inhibit translation or promote degradation, thereby influencing numerous disease processes. Certain miRNAs have been found to play significant roles in the development and progression of nephrolithiasis. Through bioinformatic analysis, this study predicts that IRF-1 may bind to the promoter region of miR-301 and potentially promote its transcription. miR-301 has been reported to regulate inflammatory responses and participate in macrophage

polarization. Notably, CSF-1 is known to promote M2 macrophage polarization, and further prediction suggests that CSF-1 is a potential downstream target of miR-301.

Based on the above background, we hypothesize that high oxalate stimuli upregulate IRF-1 expression in renal tubular epithelial cells, which in turn enhances miR-301 transcription by binding to its promoter region. Increased miR-301 inhibits CSF-1 expression, reduces M2 macrophage polarization, disrupts the M1/M2 balance, and exacerbates inflammatory responses and crystal deposition. This study aims to investigate the role of the IRF-1/miR-301/CSF-1 signaling axis in CaOx stone formation through in vitro and in vivo experiments, thereby providing new therapeutic targets and a theoretical basis for clinical prevention and treatment.

2. Materials and Methods

2.1. Cell Culture and Treatment

The human renal tubular epithelial cell line (HK-2) was purchased from Boster Biological Technology (Wuhan, China). HK-2 cells were cultured in Dulbecco's Modified Eagle Medium (DMEM, Gibco, USA) supplemented with 10% fetal bovine serum (FBS, Gibco) at 37°C in a humidified atmosphere containing 5% CO_2. To establish an in vitro hyperoxaluria model, HK-2 cells were treated with 800 μM sodium oxalate (NaOx, Sigma, USA) for 24 or 48 hours when cell confluence reached approximately 80%.

2.2. Plasmid and Oligonucleotide Transfection

The IRF-1 overexpression plasmid (pcDNA3.1-IRF-1) and its empty vector control (pcDNA3.1) were constructed by GenePharma (Shanghai, China). The miR-301 mimic, miR-301 inhibitor, and their corresponding negative controls (mimic-NC, inhibitor-NC) were also synthesized by GenePharma. All transfections were performed using Lipofectamine 3000 reagent according to the manufacturer's instructions. Briefly, 2.5 μg of plasmid or 50 nM of miRNA oligonucleotides were diluted in serum-free DMEM, mixed with Lipofectamine 3000, and then added to the cells. Cells were harvested 48 hours post-transfection for further analysis.

2.3. Co-culture System

Human monocytic THP-1 cells were differentiated into M0 macrophages by treatment with 100 ng/mL phorbol 12-myristate 13-acetate (PMA, Sigma, USA) for 48 hours. Differentiated macrophages were seeded into the upper chamber of a Transwell system. HK-2 cells subjected to various treatments were cultured in the lower chamber. The two cell types were co-cultured for 48 hours, after which macrophages in the upper chamber were collected for RNA extraction and qRT-PCR analysis of polarization markers.

2.4. Total RNA was extracted from cells or tissues using TRIzol reagent (Invitrogen, USA) according to the manufacturer's protocol.

For miRNA analysis, cDNA was synthesized using the Synthesis SuperMix Kit (Yeasen Biotechnology). qPCR was performed on a 7500 Real-Time PCR System (Biometra, Germany) using SYBR Green PCR Master Mix (Yeasen Biotechnology). The expression of target genes was normalized to GAPDH, and the expression of miR-301 was normalized to U6 snRNA. The primer sequences are shown below: miR-301 (F: 5'-CGCGCAGTGCAATAGTATTGT-3', R: 5'-AGTGCAGGGTCCGAGGTATT-3'); GAPDH (F: 5'-CAGGAGGCATTGCTGATGAT-3', R: 5'-GAAGGCTGGGGCTCATTT-3'); CD163 (F: 5'-TTTGTCAACTTGAGTCCCTTCAC-3', R: 5'-TCCCGCTACACTTGTTTTCAC-3'); CD206 (F: 5'-GGGTTGCTATCACTCTCTATGC-3', R: 5'-TTTCTTGTCTGTTGCCGTAGTT-3'); IL-1β (F: 5'-ATGATGGCTTATTACAGTGGCAA-3', R: 5'-ATGGGAGATTCGTAGCTGGA-3'); Arg1 (F: 5'-GAGGAAACTTGCATGGACAAC-3', R: 5'-AATCCTGGCACATCGGGAATC-3'); iNOS (F: 5'-TCCAGTATCACAACCTCAGCAAG-3', R: 5'-TGGACCTGCAAGTTAAAATCCC-3'); IL-6 (F: 5'-TAGTCCTTCCTACCCCAATTTCC-3', R: 5'-CCATCTTTGGAAGGTTCAGGTTG-3'); IL-10 (F: 5'-GACTTTAAGGGTTACCTGGGTTG-3', R: 5'-TCACATGCGCCTTGATGTCTG-3'); IRF-1 (F: 5'-GTCCTTGACCTAAGCCCCAT-3', R: 5'-GCCAGACTCGGGATAAAACTAC-3'); CSF-1 (F: 5'-TGGCGAGCAGGAGTATCAC-3', R: 5'-AGGTCTCCATCTGACTGTCAAT-3'); CD80 (F: 5'-ACTGGCAAGAATCCAAACCAACC-3', R: 5'-GCATTTCTGCAGGTCAGGCATGTT-3').

2.5. Western Blot Analysis. Cells were lysed using RIPA buffer (Beyotime, China) supplemented with 1 mM PMSF. Protein concentration was determined using a BCA protein assay kit (Elabscience, China). Equal amounts of protein were separated by 10% SDS-PAGE and transferred onto PVDF membranes (Millipore, USA). The membranes were blocked with 5% bovine serum albumin (BSA) for 1 hour at room temperature and then incubated overnight at 4°C with primary antibodies against IRF-1 (1:1000, Abclonal, China), CSF-1 (1:1000, Abclonal), or β-actin (1:3000, Abclonal). After washing, the membranes were incubated with HRP-conjugated secondary antibodies (1:5000, Abclonal) for 1 hour at room temperature. Protein bands were visualized using an Enhanced Chemiluminescence (ECL) kit (Boster, China) and imaged with a chemiluminescence imaging system (Bio-Rad, USA).

2.6. Dual-Luciferase Reporter Assay. The wild-type (WT) 3'-untranslated region (UTR) of CSF-1 containing the predicted miR-301 binding site and a mutant (MUT) version were synthesized and cloned into the pmirGLO dual-luciferase vector (Promega, USA). HK-2 cells were co-transfected with either the WT or MUT reporter plasmid and the miR-301 mimic or mimic-NC using Lipofectamine 3000. After 48 hours, luciferase activity was measured using the Dual-Luciferase Reporter Assay System (Promega, USA) according to the manufacturer's instructions. Firefly luciferase activity was

normalized to Renilla luciferase activity for each sample.
2.7. Animal Experiments. All animal procedures were approved by the Animal Ethics Committee of Zunyi Medical University and conducted in accordance with the NIH Guide for the Care and Use of Laboratory Animals. C57BL/6J male mice (6-8 weeks old) were bought from the experimental animal center of Zunyi Medical University(Zunyi, China) and used in the experiments.IRF-1 knockout (IRF-1−/−) mice were generated using CRISPR-Cas9 technology(GenePharma, China). To induce CaOx kidney calcification, mice were intraperitoneally injected with either normal saline or glyoxylic acid (GA) at a dose of 80 mg/kg/day from day 4 to day 10. AgomiR-301, a miR-301 agonist synthesized , was administered via tail vein injection on days 1, 4, and 7 at a dose of 20 mg/kg in 200 μL volume. Wild-type (WT) and IRF-1−/− male mice were randomly divided into the following groups (n=10 per group):Group A: WT mice + daily intraperitoneal (i.p.) injection of saline.Group B: WT mice + daily i.p. injection of GA (80 mg/kg).Group C: WT mice + daily i.p. injection of GA (80 mg/kg) + tail vein injection of agomIR-301.Group D: IRF-1−/− mice + daily i.p. injection of GA (80 mg/kg).Group E: IRF-1−/− mice + daily i.p. injection of GA (80 mg/kg) + tail vein injection of agomIR-301.On day 10, mice were euthanized, and kidney tissues were collected for analysis.
2.8. Assessment of Crystal Deposition. Kidney tissues were fixed in 4% paraformaldehyde, embedded in paraffin, and sectioned. CaOx crystal deposition was assessed by Von Kossa staining following standard protocols. The stained sections were imaged under a light microscope (Nikon, Japan), and the area of crystal deposition was quantified using Image-Fiji software.
2.9. Fluorescence In Situ Hybridization (FISH). The expression and localization of miR-301 in mouse kidney tissues were detected using an RNA FISH Kit (GenePharma, China) according to the manufacturer's instructions. Briefly, paraffin-embedded kidney sections were deparaffinized, rehydrated, and digested with proteinase K. Sections were then hybridized with a specific FITC-labeled miR-301 probe overnight at 37°C. After stringent washing, cell nuclei were counterstained with DAPI. Images were captured using a fluorescence microscope (Nikon, Japan).
2.10. Immunohistochemical (IHC). Kidney sections were deparaffinized and rehydrated. Endogenous peroxidase activity was blocked by incubation with 3% H_2O_2 for 15 minutes at room temperature. After rinsing with distilled water and phosphate-buffered saline (PBS), the sections were placed in citrate buffer (10 mM, pH 6.0) and heated in a microwave oven at 95 °C for 15 minutes for antigen retrieval.The sections were then incubated overnight at 4 °C with the following primary antibodies: rabbit anti-IRF-1 (1:100 dilution) or rabbit anti-CSF-1 (1:100 dilution). Following a PBS wash, the sections were incubated with a goat anti-rabbit IgG HRP-conjugated secondary antibody for 30 minutes at room

temperature. Antigen visualization was achieved by staining with 3,3’-diaminobenzidine (DAB). These parts were treated with oxysosome, dehydration and installation. Then images were taken using the Japanese fluorescent light field. Expression levels were calculated using Image J software, and relative expression was calculated according to the average density of light (AOD) at least five random high field fields to the segment.

2.11. Statistical Analysis.All data is expressed as the average ± standard deviation (SD). Statistical analysis is carried out using GraphPad Prism 10.0 software. The differences between the two groups were analyzed using student T-tests. Comparipose between several groups were analyzed using a one-way dispersion analysis (ANOVA) and the Tukey analysis after testing.

3. Results

3.1 High concentrations of NaOx reduce the viability of HK-2 cells and polarize macrophages M1, which are co-louced with it.

To determine the effect of high NaOx concentrations on renal cells, HK-2 cells were cultured with various concentrations of NaOx for 48 hours. Cell viability gradually decreased with increasing NaOx concentration. A significant reduction in viability was observed at 800 μM NaOx, which was therefore used in subsequent experiments to mimic the hyperoxaluric environment (Fig. 1A). A co-culture system was established (Fig. 1B). After 48 hours of co-culture, qRT-PCR analysis of macrophage markers showed that macrophages co-cultured with NaOx-stimulated HK-2 cells significantly shifted toward the M1 phenotype, as evidenced by increased expression of M1 markers (CD80, IL-1β, IL-6, iNOS) (Fig. 1C), while the expression of M2 markers (CD206, IL-10, CD163, Arg-1) was decreased compared to the control group (Fig. 1D).

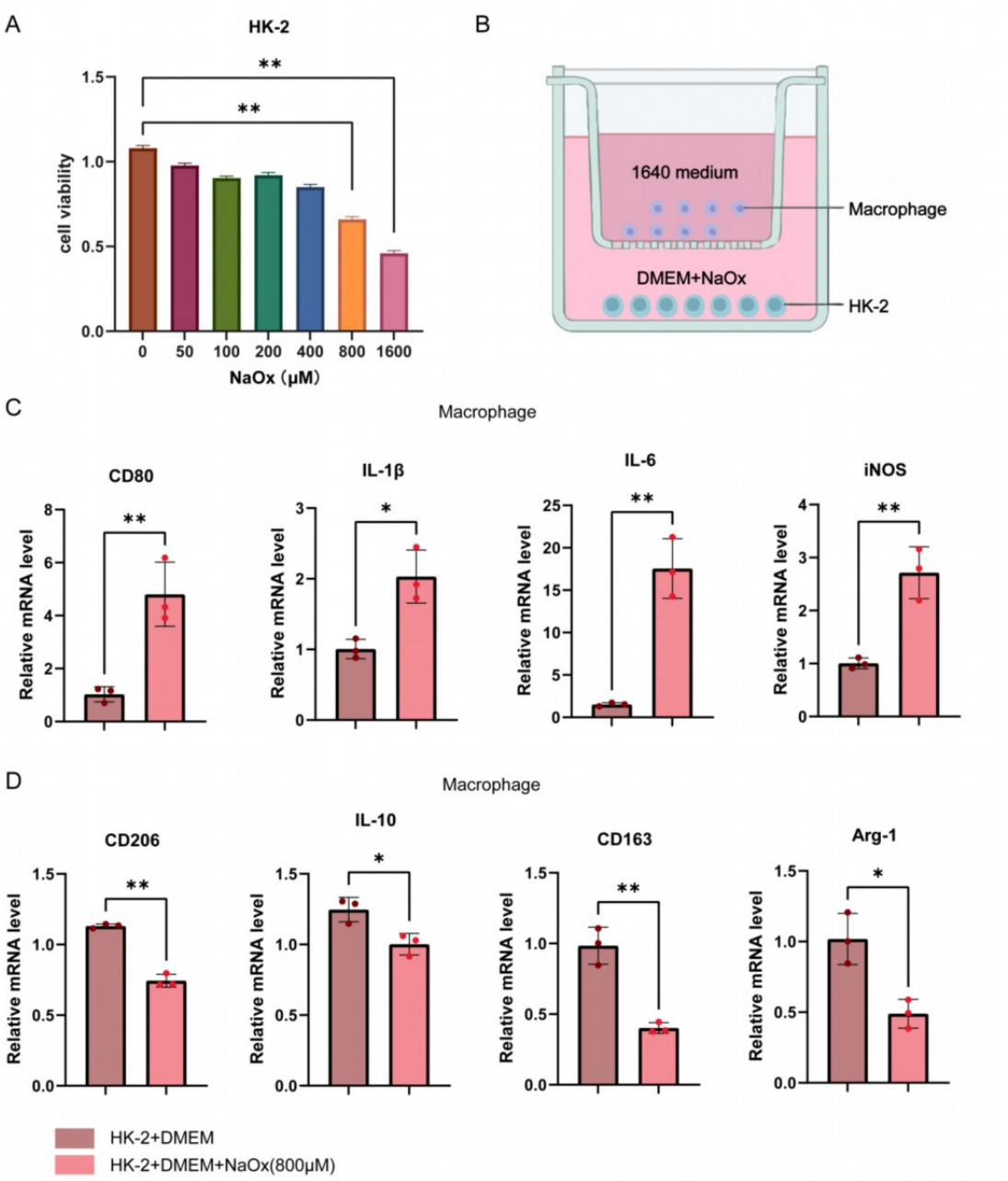

Fig. 1 High NaOx reduces HK-2 cell viability and promotes M1 macrophage polarization.(A) CCK-8 assay of HK-2 cell viability after 48 h culture with different concentrations of NaOx. (B) Schematic diagram of the co-culture system of HK-2 cells with macrophages. (C) qRT-PCR analysis of M1 macrophage markers (CD80, IL-1β, IL-6, iNOS) in macrophages co-cultured with high-concentration NaOx-stimulated HK-2 cells. (D) qRT-PCR analysis of M2 macrophage markers (CD206, IL-10, CD163, Arg-1) in macrophages co-cultured with high-concentration NaOx-stimulated HK-2 cells. *P < 0.05, **P < 0.01 vs. control group.

3.2 High NaOx induced the upregulation of IRF-1 in HK-2 cells.

Given that HK-2 cells promote M1 macrophage polarization under high NaOx stimulation, we cultured HK-2 cells with 800 μM NaOx for 24 and 48 hours. IRF-1 expression was measured by Western blot

and qRT-PCR. Western blot analysis showed a time-dependent increase in IRF-1 protein levels following NaOx treatment (Fig. 2A, 2B). This upregulation was confirmed at the mRNA levels by qRT-PCR (Fig. 2C).

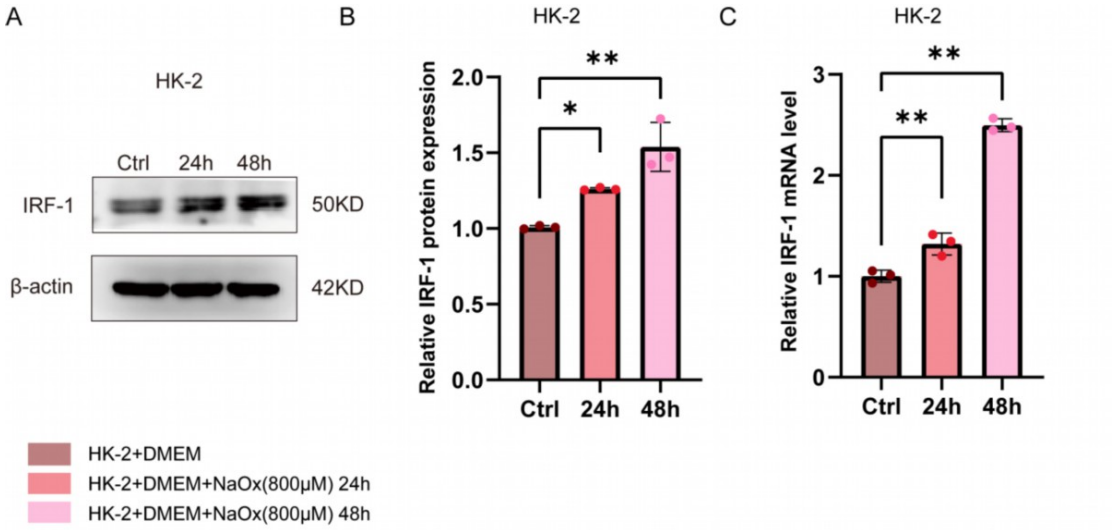

Fig. 2 High NaOx induces upregulation of IRF-1 in HK-2 cells.(A, B) Western blot analysis of IRF-1 protein expression in HK-2 cells after 24 h and 48 h of high-concentration NaOx stimulation. (C) qRT-PCR analysis of IRF-1 mRNA expression in HK-2 cells after 24 h and 48 h of high-concentration NaOx stimulation. *P < 0.05, **P < 0.01 vs. control group.

3.3 Upregulation of IRF-1 in HK-2 cells drove M1 macrophage polarization under high NaOx conditions.

To investigate the role of IRF-1 upregulation in macrophage polarization, we constructed an IRF-1 overexpression plasmid. A co-culture system was established in which HK-2 cells transfected with IRF-1 overexpression plasmid or empty vector were treated with 800 μM NaOx and co-cultured with macrophages (Fig. 3A). Transfection with pcDNA3.1-IRF-1 increased IRF-1 expression at both the protein (Fig. 3B, 3C) and mRNA levels (Fig. 3D). Under high oxalate conditions, IRF-1-overexpressing HK-2 cells promoted M1 polarization, as shown by elevated M1 marker expression (Fig. 3E) and reduced M2 markers expression(Fig. 3F).

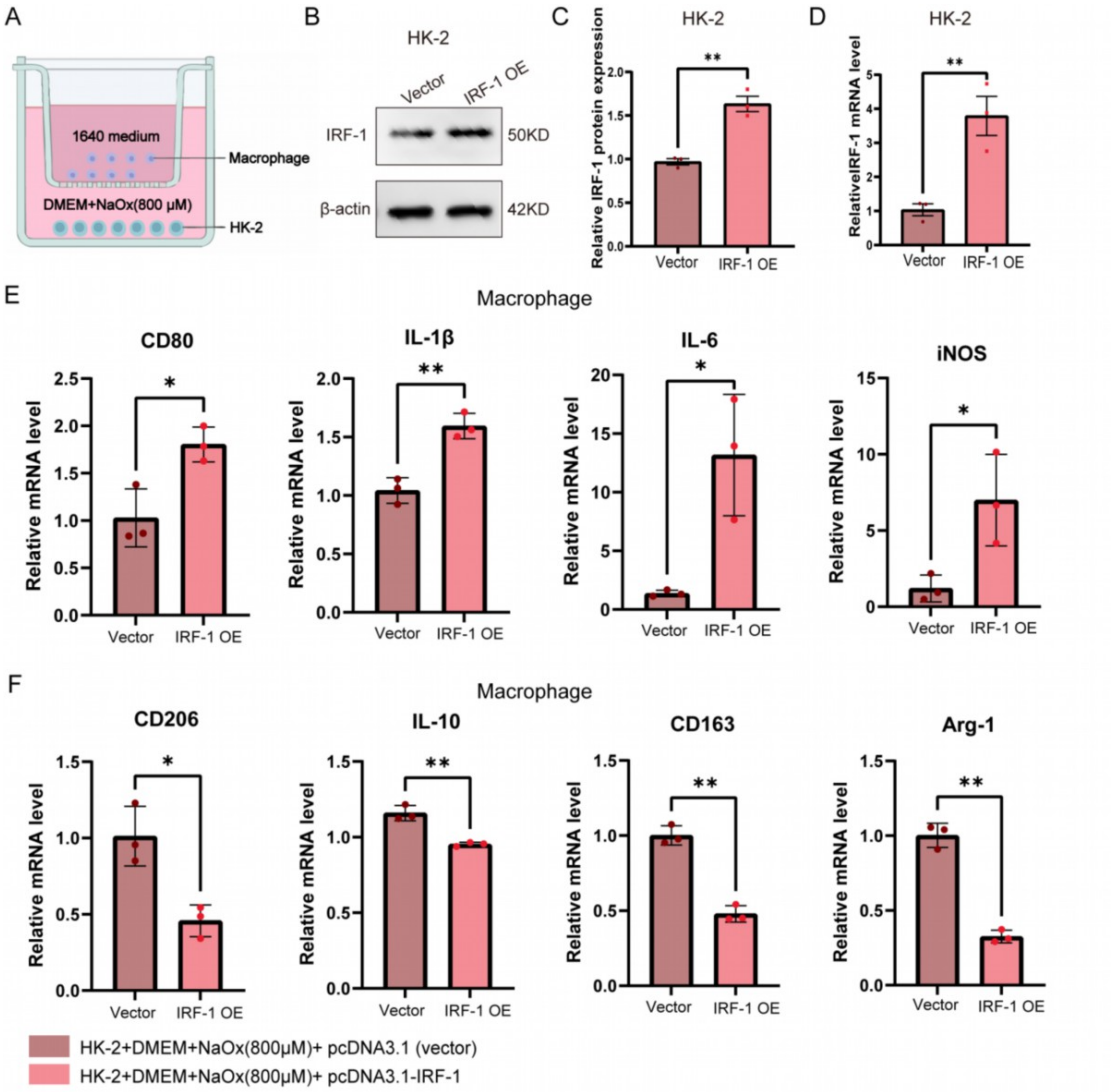

Fig. 3 Upregulation of IRF-1 in HK-2 cells drives M1 macrophage polarization under high NaOx conditions.(A) Schematic diagram of the co-culture system. (B, C) Western blot analysis and quantification of IRF-1 protein expression following IRF-1 overexpression. (D) qRT-PCR analysis of IRF-1 mRNA expression following IRF-1 overexpression. (E) qRT-PCR analysis of M1 macrophage markers. (F) qRT-PCR analysis of M2 macrophage markers. *P < 0.05, **P < 0.01 vs. Vector group.

3.4 NaOx stimulation upregulated miR-301 and downregulated CSF-1 via IRF-1 in HK-2 cells.

We assessed miR-301 and CSF-1 expression in HK-2 cells after NaOx exposure. NaOx treatment downregulated CSF-1 protein and mRNA levels in a time-dependent manner (Fig. 4A–4C) while upregulating miR-301 expression (Fig. 4D). Bioinformatics analysis

predicted miR-301-3p as a transcriptional target of IRF-1 (Fig. 4E). IRF-1 overexpression further enhanced miR-301 levels (Fig. 4F) and suppressed CSF-1 expression at both mRNA and protein levels (Fig. 4G–4I). These results indicate that NaOx upregulates miR-301 and downregulates CSF-1 via an IRF-1-mediated pathway.

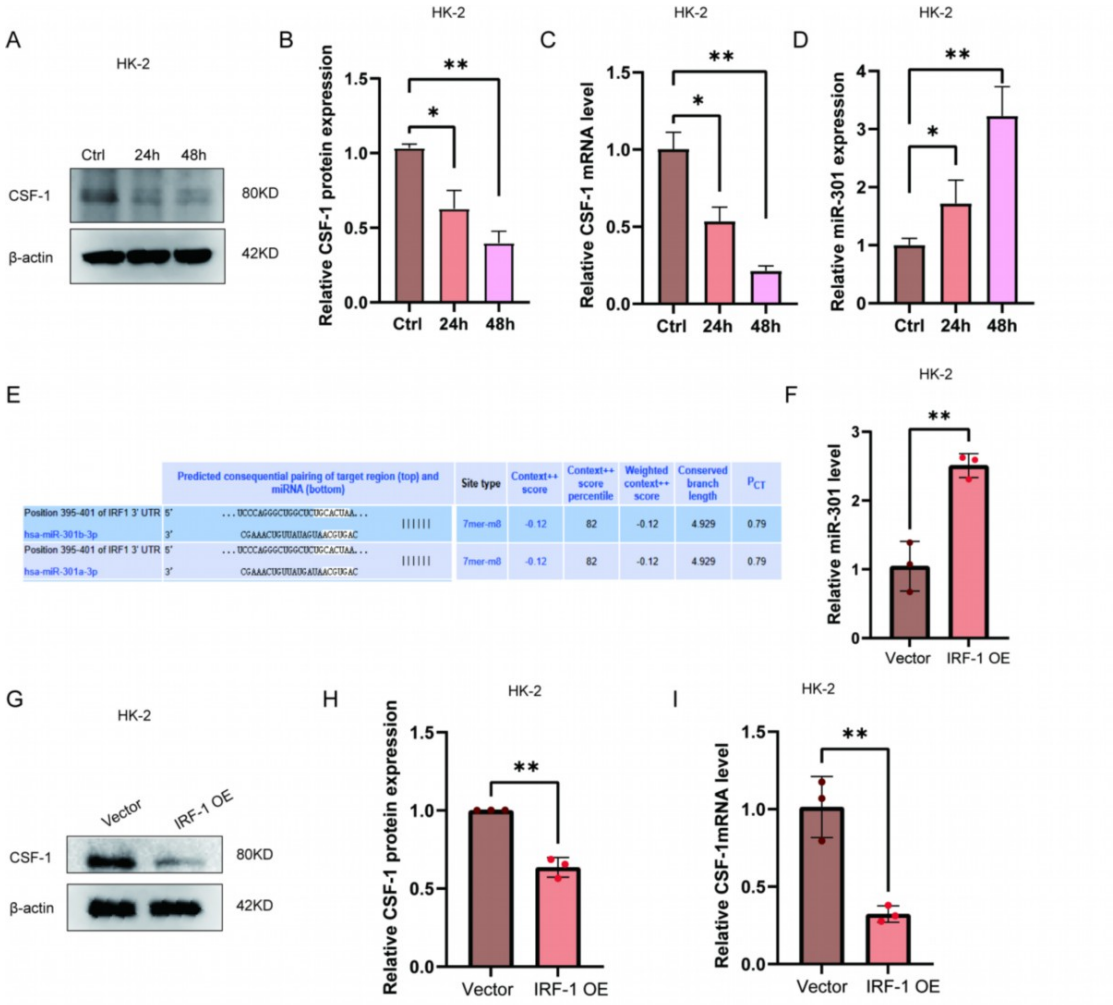

Fig. 4 NaOx stimulation upregulates miR-301 and downregulates CSF-1 via IRF-1.(A, B) Western blot analysis of CSF-1 protein expression in HK-2 cells stimulated with NaOx for 24 h and 48 h. (C, D) qRT-PCR analysis of CSF-1 and miR-301 expression. (E) Predicted binding sites of IRF-1 in the miR-301 promoter. (F) qRT-PCR analysis of miR-301 expression following IRF-1 overexpression. (G–I) Western blot and qRT-PCR analysis of CSF-1 expression following IRF-1 overexpression. *P < 0.05, **P < 0.01 vs. control or Vector group.

3.5 CSF-1 was a direct target gene of miR-301.

Bioinformatic analysis using TargetScan predicted CSF-1 as a potential downstream target of miR-301 (Fig. 5A). A dual-luciferase reporter assay demonstrated that miR-301 significantly suppressed the activity of the wild-type CSF-1 3′-UTR reporter but not that of the mutant construct (Fig. 5B). Western blot analysis showed that miR-301 overexpression reduced CSF-1 protein levels, while miR-301 inhibition enhanced CSF-1 expression in HK-2 cells under NaOx treatment (Fig. 5C, 5D). These results confirm that CSF-1 is a direct functional target of miR-301.

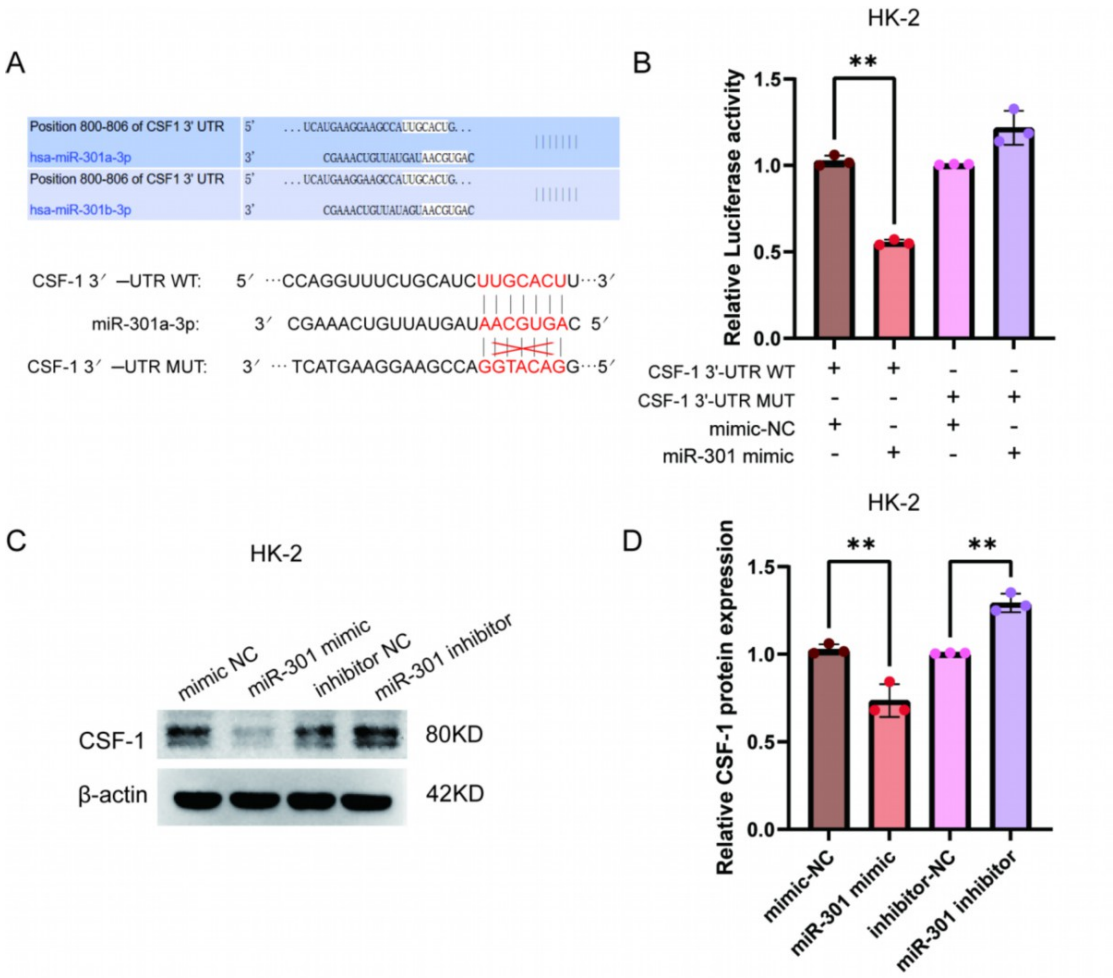

Fig. 5 CSF-1 is a direct target gene of miR-301.(A) Predicted binding sites between miR-301 and CSF-1, with schematic representation of wild-type and mutant seed sequences. (B) Luciferase reporter assay in HK-2 cells co-transfected with WT or mutant CSF-1 3′-UTR reporters and miR-301 mimics or NC. (C, D) Western blot analysis of CSF-1 expression in HK-2 cells treated with NaOx and transfected with

miR-301 mimics, inhibitors, or controls. *P < 0.05, **P < 0.01 vs. NC group.

3.6 Macrophage polarization was regulated by CSF-1.

Recombinant CSF-1 directly applied to macrophages increased the expression of M2 markers (Fig. 6A), confirming its role in promoting M2 polarization. Using a Transwell co-culture system (Fig. 6C, 6F), miR-301 mimic-transfected HK-2 cells promoted M1 marker expression in co-cultured macrophages (Fig. 6B), whereas miR-301 inhibitor increased M2 marker expression (Fig. 6D). Rescue experiments showed that recombinant CSF-1 reversed the M1-promoting effect of miR-301 mimic (Fig. 6E, 6G). Thus, miR-301 promotes M1 macrophage polarization by targeting and downregulating CSF-1.

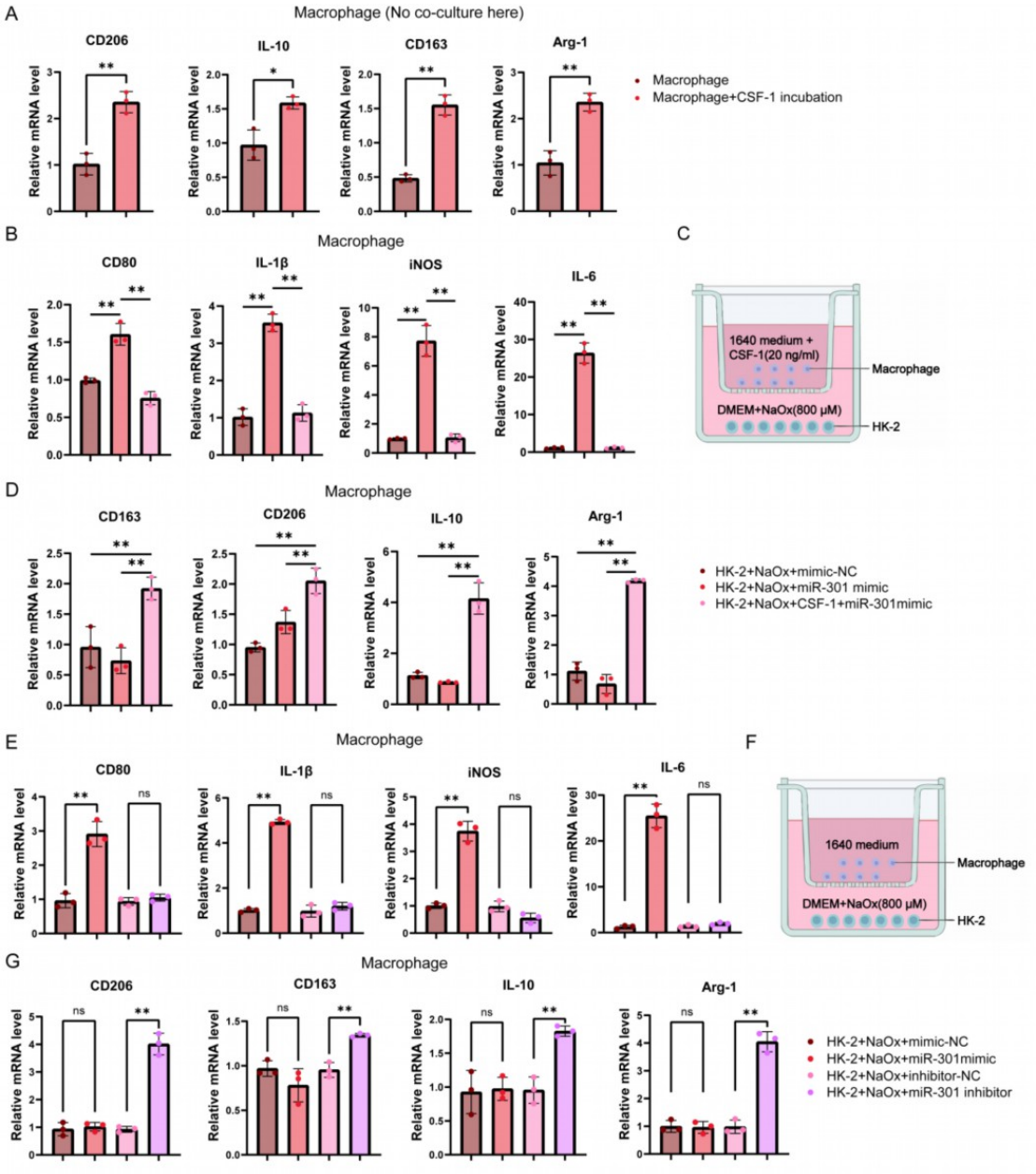

Fig. 6 miR-301 promotes M1 macrophage polarization by targeting CSF-1.(A) qRT-PCR analysis of M2 markers in macrophages treated with recombinant CSF-1. (B, D) qRT-PCR analysis of M1 markers (B) and M2 markers (D) in macrophages co-cultured with HK-2 cells transfected with miR-301 mimic or inhibitor. (C, F) Schematic diagrams of the Transwell co-culture systems. (E, G) qRT-PCR analysis of M1 markers (E) and M2 markers (G) in macrophages co-cultured with HK-2 cells treated with miR-301 mimic alone or in combination with recombinant CSF-1. *P < 0.05, **P < 0.01.

3.7 The IRF-1/miR-301/CSF-1 axis promotes renal calcium oxalate crystal formation in mice.

Compared to the control group, GA-treated mice showed increased CaOx crystal deposition (Fig. 7B), elevated miR-301 expression (Fig. 7A) and IRF-1 expression (Fig. 7C), and reduced

CSF-1 expression (Fig. 7D). AgomiR-301 administration further enhanced crystal deposition, increased miR-301 and IRF-1 levels, and further decreased CSF-1 expression in GA-treated mice. In IRF-1 knockout mice, crystal deposition was reduced, accompanied by lower miR-301 and IRF-1 expression and restored CSF-1 levels. Moreover, agomiR-301 treatment partially reversed the protective effect of IRF-1 knockout, increasing crystal deposition, upregulating miR-301, and decreasing CSF-1 expression. These in vivo findings are consistent with the cellular results, supporting that the IRF-1/miR-301/CSF-1 axis regulates CaOx crystal formation under hyperoxaluric conditions.

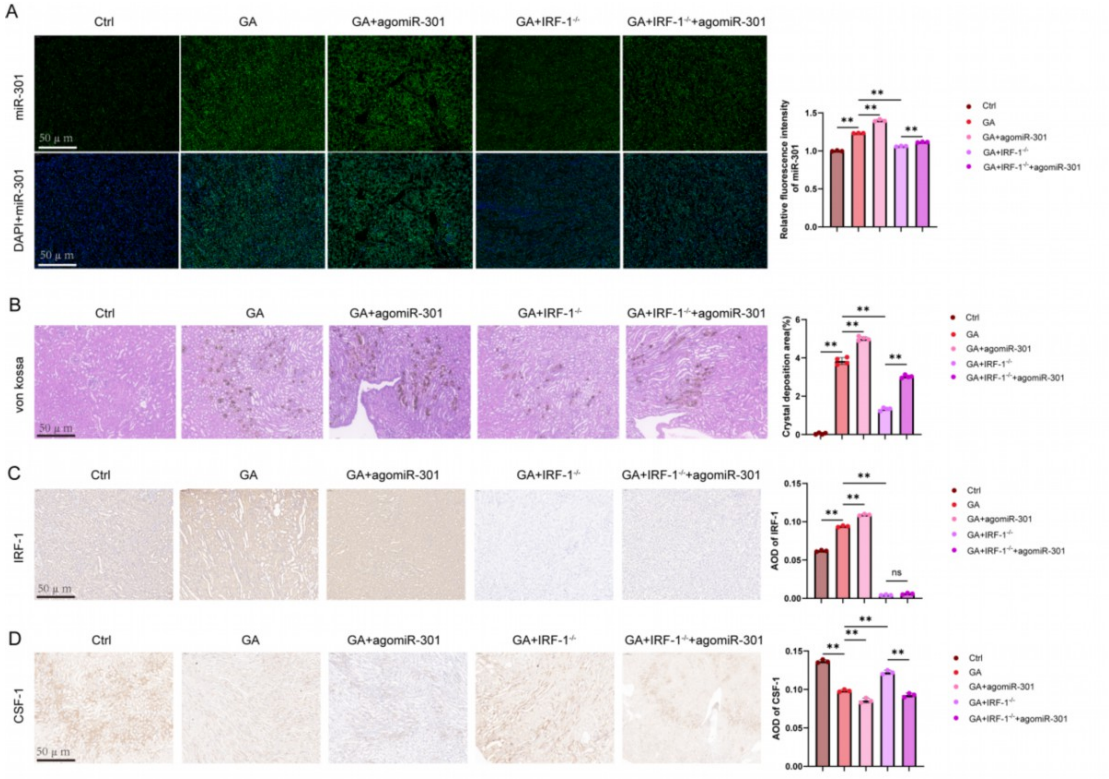

Fig. 7 The IRF-1/miR-301/CSF-1 axis contributes to CaOx crystal formation in mice.(A) FISH detection of miR-301 expression in different groups. (B) Von Kossa staining for CaOx crystal deposition. (C, D) Immunohistochemical staining of IRF-1 and CSF-1 expression. *P < 0.05, **P < 0.01: GA vs. Ctrl; GA + agomiR-301 vs. GA; GA + IRF-1^{-}/$^{-}$ vs. GA; GA + IRF-1^{-}/$^{-}$ + agomiR-301 vs. GA + IRF-1^{-}/$^{-}$.

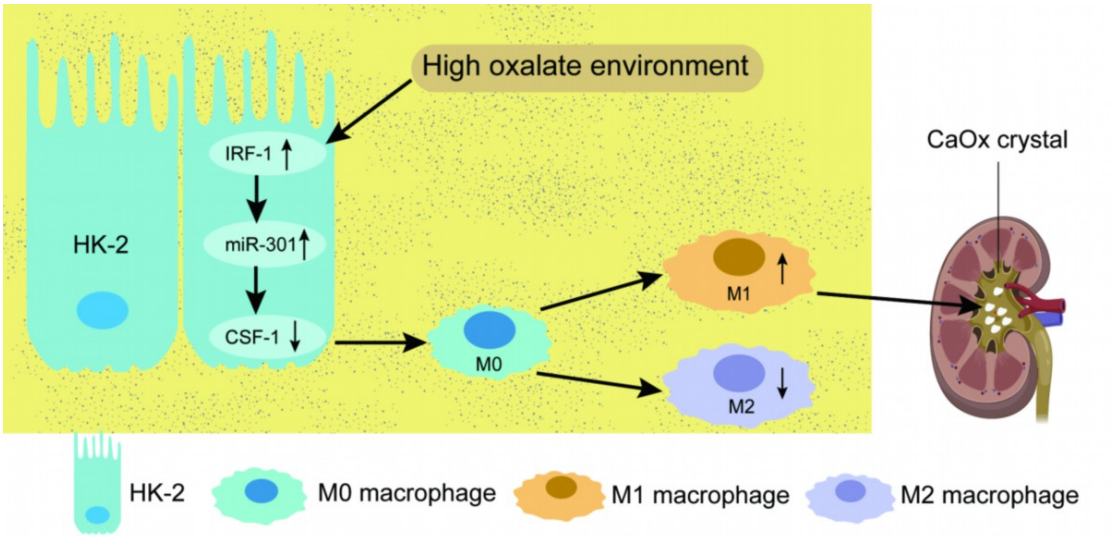

Fig. 8 Schematic model of the proposed signaling pathway. Hyperoxaluria stimulates renal tubular epithelial cells (HK-2) to upregulate IRF-1 expression, which increases miR-301 transcription. Elevated miR-301 directly targets and suppresses CSF-1 expression. Decreased CSF-1 disrupts the M1/M2 balance, promoting M1 polarization and ultimately facilitating CaOx crystal deposition.

4.Discussion

Calcium oxalate stones account for more than 80% of all kidney stone cases. The traditional view emphasizes supersaturation of oxalate and calcium ions in the urine. However, recent studies have shown that crystal adhesion to renal tubular epithelial cells, aggregation, and subsequent local damage and inflammatory responses are critical for stone formation. In a hyperoxaluric environment, the IRF-1/miR-301/CSF-1 axis promotes M1 macrophage polarization and accelerates CaOx crystal deposition in the kidneys. Our findings provide a better understanding of the interaction between renal tubular epithelial cells and macrophages in CaOx nephrolithiasis.

In this study, NaOx exposure reduced HK-2 cell viability in a concentration-dependent manner, with a significant effect at 800 μM, indicating that elevated oxalate levels are key to renal cell injury. Furthermore, high NaOx not only affected tubular epithelial cells but also promoted pro-inflammatory responses. Increased M1 macrophage infiltration was closely associated with the degree of kidney injury, consistent with previous reports on NaOx-induced inflammation.

Mechanistically, IRF-1 plays a crucial role in the hyperoxaluric environment. IRF-1 is an important transcription factor that regulates

immune and inflammatory responses. NaOx stimulation significantly increased IRF-1 expression, which correlated with elevated M1 macrophage markers, suggesting that IRF-1 promotes NaOx-induced renal inflammation by facilitating M1 polarization. Thus, IRF-1 may represent a novel therapeutic target for regulating nephritis.

We further investigated the relationship between IRF-1, miR-301, and CSF-1. NaOx exposure upregulated miR-301 and downregulated CSF-1. CSF-1 is a key factor in macrophage polarization that typically promotes M2 polarization and reduces inflammation. The increase in miR-301 by NaOx inhibits CSF-1, indicating that miR-301 acts as a negative regulator of CSF-1 in NaOx-induced nephritis.

Using a dual-luciferase reporter assay, we confirmed that miR-301 directly targets the 3′-UTR of CSF-1. Through this mechanism, miR-301 not only regulates macrophage polarization but also plays a key role in NaOx-induced kidney injury. This finding clarifies how miR-301 modulates the renal immune response in hyperoxaluria by targeting CSF-1, thereby affecting stone formation.

Importantly, supplementation with recombinant CSF-1 shifted macrophage differentiation toward the M2 phenotype, suggesting that CSF-1 alleviates NaOx-induced inflammation. Thus, CSF-1 acts as an immune regulator that counteracts M1 polarization in a high-oxalate environment and attenuates nephritis. This raises the possibility that modulating CSF-1 levels could regulate immune responses and prevent further kidney injury.

Our in vivo experiments using a CaOx nephrolithiasis mouse model strongly support the cellular findings. CaOx crystal deposition in the kidneys was associated with increased IRF-1 and miR-301 expression and decreased CSF-1 expression. IRF-1 knockout mice exhibited reduced crystal deposition and restored CSF-1 levels, further confirming the role of IRF-1 in NaOx-induced kidney injury. Notably, administration of agomiR-301 to IRF-1 knockout mice significantly increased CaOx crystal deposition, indicating that excessive activation of miR-301 can counteract the effects of IRF-1 deficiency and promote stone formation.

In summary, this study details the molecular mechanism by which NaOx induces kidney injury and macrophage polarization, focusing on the interaction among IRF-1, miR-301, and CSF-1. IRF-1 regulates miR-301 and CSF-1, driving M1 macrophage polarization, which exacerbates nephritis and stone formation. Targeting this molecular pathway may open new avenues for the treatment of CaOx kidney stones and other related kidney diseases, particularly in patients with hyperoxaluria.

5.Conclusion

The IRF-1/miR-301/CSF-1 signaling axis plays a critical role in hyperoxaluria-induced renal injury by promoting M1 macrophage polarization and calcium oxalate crystal deposition. These findings provide a new mechanistic insight into CaOx stone formation and suggest that targeting this axis may represent a novel therapeutic strategy for prevention and treatment.

References

[1]. Sáenz-Medina J, San Román J, Rodríguez-Monsalve M, et al. Hospitalization Burden of Patients with Kidney Stones and Metabolic Comorbidities in Spain during the Period 2017-2020. Metabolites. 2023 Apr 18;13(4):574.

[2]. Zeng G, Mai Z, Xia S, et al. Prevalence of kidney stones in China: an ultrasonography based cross-sectional study. BJU Int. 2017 Jul;120(1):109-116.

[3]. Siener R. Nutrition and Kidney Stone Disease. Nutrients. 2021 Jun 3;13(6):1917.

[4]. Peerapen P, Thongboonkerd V. Kidney Stone Prevention. Adv Nutr. 2023 May;14(3):555-569.

[5]. Cochat P, Rumsby G. Primary hyperoxaluria. N Engl J Med. 2013 Aug 15;369(7):649-58.

[6]. Moe OW, Xu LHR. Hyperuricosuric calcium urolithiasis. J Nephrol. 2018 Apr;31(2):189-196.

[7]. Siener R, Bangen U, Sidhu H, et al. The role of Oxalobacter formigenes colonization in calcium oxalate stone disease. Kidney Int. 2013 Jun;83(6):1144-9.

[8]. Liu YD, Yu SL, Wang R, et al. Rosiglitazone Suppresses Calcium Oxalate Crystal Binding and Oxalate-Induced Oxidative Stress in Renal Epithelial Cells by Promoting PPAR-γ Activation and Subsequent Regulation of TGF-β1 and HGF Expression. Oxid Med Cell Longev. 2019 Nov 12;2019:4826525.

[9]. Narula S, Tandon S, Kumar D, et al. Human kidney stone matrix proteins alleviate hyperoxaluria induced renal stress by targeting cell-crystal interactions. Life Sci. 2020 Dec 1;262:118498.

[10]. Mulay SR, Eberhard JN, Desai J, et al. Hyperoxaluria Requires TNF Receptors to Initiate Crystal Adhesion and Kidney Stone Disease. J Am Soc Nephrol. 2017 Mar;28(3):761-768.

[11]. Suryavanshi MV, Bhute SS, Jadhav SD, et al. Hyperoxaluria leads to dysbiosis and drives selective enrichment of oxalate metabolizing bacterial species in recurrent kidney stone endures. Sci Rep. 2016 Oct 6;6:34712.

[12]. Ivanovski O, Drüeke TB. A new era in the treatment of calcium oxalate stones? Kidney Int. 2013 Jun;83(6):998-1000.

[13]. Carney EF. Stones: TNFRs mediate CaOx deposition in hyperoxaluria. Nat Rev Nephrol. 2016 Nov;12(11):651.

[14]. Khan SR, Canales BK, Dominguez-Gutierrez PR. Randall's plaque and calcium oxalate stone formation: role for immunity and inflammation. Nat Rev Nephrol. 2021 Jun;17(6):417-433.

[15]. Robertson WG, Peacock M, Nordin BE. Calcium oxalate crystalluria and urine saturation in recurrent renal stone-formers. Clin Sci. 1971 May;40(5):365-74.

[16]. Mulay SR, Shi C, Ma X, et al. Novel Insights into Crystal-Induced Kidney Injury. Kidney Dis (Basel). 2018 Jun;4(2):49-57.
[17]. Khan SR. Reactive oxygen species, inflammation and calcium oxalate nephrolithiasis. Transl Androl Urol. 2014 Sep 1;3(3):256-276.
[18]. Yao R, Pan JS, He RB,et al. Pectolinarigenin alleviates calcium oxalate-induced renal inflammation and oxidative stress by binding to HIF-1α. Int Immunopharmacol. 2024 Dec 25;143(Pt 1):113284.
[19]. Dominguez-Gutierrez PR, Kwenda EP, Khan SR,et al. Immunotherapy for stone disease. Curr Opin Urol. 2020 Mar;30(2):183-189.
[20]. Murray PJ. Macrophage Polarization. Annu Rev Physiol. 2017 Feb 10;79:541-566.
[21]. Taguchi K, Okada A, Hamamoto S,et al. M1/M2-macrophage phenotypes regulate renal calcium oxalate crystal development. Sci Rep. 2016 Oct 12;6:35167.
[22]. Chistiakov DA, Myasoedova VA, Revin VV, et al. The impact of interferon-regulatory factors to macrophage differentiation and polarization into M1 and M2. Immunobiology. 2018 Jan;223(1):101-111.
[23]. Chen Z, Yuan P, Sun X,et al. Pioglitazone decreased renal calcium oxalate crystal formation by suppressing M1 macrophage polarization via the PPAR-γ-miR-23 axis. Am J Physiol Renal Physiol. 2019 Jul 1;317(1):F137-F151.
[24]. Lu TX, Rothenberg ME. MicroRNA. J Allergy Clin Immunol. 2018 Apr;141(4):1202-1207.
[25]. Jiang K, Hu J, Luo G, et al. miR-155-5p Promotes Oxalate- and Calcium-Induced Kidney Oxidative Stress Injury by Suppressing MGP Expression. Oxid Med Cell Longev. 2020 Mar 4;2020:5863617.
[26]. Zhu W, Zhou Z, Wu C, et al. miR-148b-5p regulates hypercalciuria and calcium-containing nephrolithiasis. Cell Mol Life Sci. 2024 Aug 25;81(1):369.
[27]. Li Y, Fu Z, Deng C, et al. miR-301a-5p regulated IKKβ/NF-κB axis and macrophage polarization to accelerate skin wound healing. Int J Biol Macromol. 2025 Jun;311(Pt 4):143995.
[28]. Vogel DY, Glim JE, Stavenuiter AW, et al. Human macrophage polarization in vitro: maturation and activation methods compared. Immunobiology. 2014 Sep;219(9):695-703.
[29]. Kachkoul R, Touimi GB, El Mouhri G,et al. Urolithiasis: History, epidemiology, aetiologic factors and management. Malays J Pathol. 2023 Dec;45(3):333-352.
[30]. Tamborino F, Cicchetti R, Mascitti M, et al. Pathophysiology and Main Molecular Mechanisms of Urinary Stone Formation and Recurrence. Int J Mol Sci. 2024 Mar 6;25(5):3075.
[31]. Ye Z, Xia Y, Li L, et al. p53 deacetylation alleviates calcium oxalate deposition-induced renal fibrosis by inhibiting ferroptosis. Biomed Pharmacother. 2023 Aug;164:114925.
[32]. Pan P, Cheng J, Si Y, et al. A stop-flow comprehensive two-dimensional HK-2 and HK-2/CIKI cell membrane chromatography comparative analysis system for screening the active ingredients from Pyrrosia calvata (Bak.) Ching against crystal-induced kidney injury. J Pharm Biomed Anal. 2021 Feb 20;195:113825.
[33]. Rudtanatip T, Phanphak J, Somintara S, et al. Effect of Gracilaria fisheri sulfated galactan with increased sulfation on cell migration and expression of cell adhesion molecules in sodium oxalate-induced HK-2 cell injury. Biomed Rep. 2025 May

22;23(2):123.
[34]. Geng F, Chen J, Song B, et al. Chaperone- and PTM-mediated activation of IRF1 tames radiation-induced cell death and the inflammatory response. Cell Mol Immunol. 2024 Aug;21(8):856-872.
[35]. Gomes MTR, Guimarães ES, Oliveira SC. ZBP1 senses Brucella abortus DNA triggering type I interferon signaling pathway and unfolded protein response activation. Front Immunol. 2025 Jan 9;15:1511949.
[36]. Fleetwood AJ, Lawrence T, Hamilton JA, et al. Granulocyte-macrophage colony-stimulating factor (CSF) and macrophage CSF-dependent macrophage phenotypes display differences in cytokine profiles and transcription factor activities: implications for CSF blockade in inflammation. J Immunol. 2007 Apr 15;178(8):5245-52.
[37]. Sierra-Filardi E, Puig-Kröger A, Blanco FJ,et al. Activin A skews macrophage polarization by promoting a proinflammatory phenotype and inhibiting the acquisition of anti-inflammatory macrophage markers. Blood. 2011 May 12;117(19):5092-101.
[38]. Yuan Y, Li Y, Zhao W, et al. WNT4 promotes macrophage polarization via granulosa cell M-CSF and reduces granulosa cell apoptosis in endometriosis. Cytokine. 2023 Dec;172:156400.

Funding
1.National Natural Science Foundation of China (Grant number: 82560155)
2.Science and Technology Fund Project of Guizhou Provincial Health Commission (Grant number: gzwkj2024-384)